3D fs-laser structuring of novel electrode materials for fuel cells

Patrick Faubert[1#], Claas Müller[1], Holger Reinecke[1], and Peter Smyrek[2], Johannes Proell[2], Wilhelm Pfleging[2,3]

1 Laboratory for Process Technology, IMTEK - Department for Microsystems Engineering, University of Freiburg, 79110 Freiburg, Germany
2 Institute for Applied Materials, Karlsruhe Institute of Technology, Germany
3 Karlsruhe Nano Micro Facility, H.-von-Helmholtz-Platz, Germany
Corresponding Author / E-mail: patrick.faubert@imtek.uni-freiburg.de, TEL: +49 (0)761 / 203-7359
Fax: +49 (0)761 / 203-7352

KEYWORDS : Non-noble electrode, Ultrafast laser structuring, Femtosecond laser, 3D architecture, Fuel cell, Energy materials

The scalable storage of renewable energy by means of converting water to hydrogen fuels electrochemically hinges on fundamental improvements in catalytic materials. For these kinds of applications, the ultimate power supply should be a self-renewing energy source. This strategy is pursued by the concept of Micro Energy Harvesting. Alkaline polymer electrolyte fuel cells have been increasingly recognized as a solution to overcome the dependence on noble metal catalysts. The key challenge is to increase the exchange current density of chromium decorated nickel electrodes by enhancement of the active surface area of the electrode itself. In this paper, we present an advanced ultrafast laser structuring technique forming three-dimensional (3D) microstructures directly into the active material. Femtosecond laser ablation allows for precise material removal without changing the material properties due to minimized heat input. By applying this advanced laser-based structuring technique, 3D microstructures be formed for an increase in active surface area. Ongoing studies will focus on investigation of exchange current density by applying both unstructured and 3D structured Cr-Ni electrodes.

NOMENCLATURE

a = edge length
h = height of a single microstructure
g = gap between the microstructures
E = potential
j = current density

1. Introduction

The scalable storage of renewable energy by means of converting water (H_2O) to hydrogen fuels (H_2) electrochemically hinges on fundamental improvements in catalytic materials. Unfortunately, as the outer system dimensions continuously decreases, less and less space is available for integrated batteries and therefore, the amount of energy storage capacity will remain finite [1]. Unlike the devices relying on a proton exchange membrane (PEM), it is possible to use an accumulator with an alkaline anion exchange membrane (AAEM) to separate the anode from the cathode. This change in pH allows both, the usage of a standard AB5/$LaNi_5$ type hydrogen storage as well as a precious-metal free bifunctional oxygen catalyst instead of platinum. There are more or less three major challenges in the development of a catalyst for the air-breathing electrode. First of all the catalyst has to show good bifunctional catalytic activity. Additionally, it has to be stable against oxidation or other degradation mechanisms. Finally the structure of the catalyst is of paramount importance as it has to provide a high amount of triple phase boundary (TPB) at a high electrical conductivity. The faster kinetics of the oxygen reduction reaction in alkaline cell provides the use of non-noble metal electrocatalysts. Therefore, it makes sense to evaluate the electrochemical operations of the anion fuel cells (AFCs) in specific areas of the relationship between cell potential, E and current density, j [2]. One main goal is to replace noble metal

catalysts like Pt in order to avoid increasing costs hampering the widespread application of fuel cells. A good overview of hydrogen evolution reaction (HER) catalysis by Trasatti contains an exhaustive description of available heterogeneous catalysts [3]. Another very interesting approach is the *ab initio* quantum chemistry study focused on studies by density functional theory (DFT) an *ab initio* molecular dynamics (AIMD) for fuel cell catalysts by calculating adsorption geometry, energy, dissociation energy barrier, reversible potential, activation energy and potential dependent properties for elementary electron transfer steps in order to illustrate the potential of these method identifying better electro catalysts [4–17]. There are also other methods of electrochemistry, such as wave-function-based method, Monte Carlo method and semi-empirical method [18,19]. Lu et al. [20] e.g., use a nonprecious metal, chromium-decorated nickel catalyst for the anode side and a silver catalyst for the cathode side. Based on DFT calculations, they found out that there are tremendous different impacts of H adsorption and O adsorption on the local density of states (LDOS) of the Ni surface by using transition metals like chromium oxide. This clearly presents the success of weakening the Ni-O bond strength and furthermore an activation of the chromium decorated nickel nanoparticles (CDN) by gaseous hydrogen at room temperature.

In this paper we describe a novel approach for increasing the exchange current density j of electrodes by enhancing the active surface area A of the electrode itself. Therefore, three-dimensional (3D) microstructures such as 3D micro-grids and micro-channel structures were formed directly into the electrode by applying an ultrafast laser ablation process.

2. Experimental

2.1 Electrode preparation

The carbon black powder (BET surface area 250 m² / g) was wetted in ethanol and poured into precursor solution. The solution was prepared by dissolving 12.13 g of $NiCl_2 \cdot 6H_2O$ and 0.314 g of $CrCl_3 \cdot 6H_2O$ in 200 ml pure water. Then 114 ml of 5 wt% KBH_4 solution was added drop-wise into the suspension at 10 °C followed by stirring for 30 min (Fig. 1a). The obtained black powder was repeatedly washed with pure water and filtered by vacuum pump until no Cl^- existed anymore. A Cl^--test with silver nitrate revealed no milky stain. Then the powder was dried in vacuum for 1 h at 900 °C heated under N_2 atmosphere. This powder was embedded into an OH-permeable ionomere-suspension (Fumatech FAA-3, 20 wt% / 80 wt% carbon black). The main function of the ionomere was to act like a binder for the catalyst powder, which likewise constitutes the functionality of the O_2 permeable sealing against exhaust of electrolyte. This mixture was screen printed on carbon paper sample of 5 x 5 cm² (Quintech,TP-120-T, Toray Paper) with a thickness of 370 µm followed by drying on the hotplate at 60 °C for 10 min and pressed at room temperature for 3 min under a pressure of 500 N cm^{-2}.

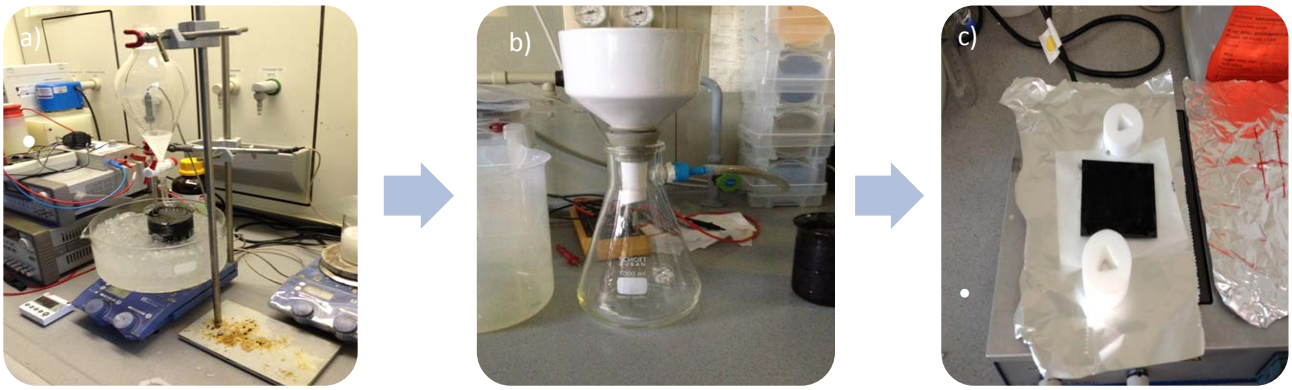

Fig. 1: Process flow (a) 114 ml of 5 wt% KBH4 solution was added drop-wise into the suspension at 10 °C followed by stirring for 30 min. (b) The obtained black powder was repeatedly washed with pure water and filtered by vacuum pump until no Cl- exists anymore. (c) This mixture was screen printed on carbon paper sample of 5 x 5 cm² (Quintech,TP-120-T, Toray Paper) with 370 µm thickness.

2.2 Electrode modification

3D microstructures were processed into electrode materials using a laser micromachining workstation of type PS450-TO (Optec s.a., Belgium) equipped with a tunable fiber laser (Tangerine, Amplitude Systemes, France). The maximum average laser power was 20 W and the maximum laser pulse energy was 100 µJ at 1030 nm (TEM_{00} with $M^2 < 1.3$). The laser pulse duration can be varied ranging from 330 fs up to 10 ps. The second harmonic (SHG) and third harmonic generation (THG) can be set by a frequency multiplier. The laser structuring process was performed for achieving both 3D

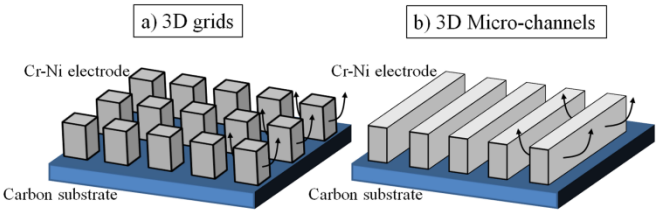

Fig. 2: Schematic drawing of laser-generated (a) 3D micro-grids and (b) 3D micro-channels in Cr-Ni electrodes coated onto carbon paper substrate.

micro-grids (Fig. 2a) and line structures (Fig. 2b) by applying a laser wavelength of 515 nm, a laser pulse repetition rate of 200 kHz, an average laser power of 0.8 W at the sample surface and a laser pulse duration of 350 fs. In order to process micro-features directly into the electrode material with a sample footprint of 5 cm x 5 cm, the laser beam was scanned over the sample surface with a scanning velocity of 500 mm/s. The pitch in between two line scans was maintained at 100 µm. The laser structuring process was carried out under ambient air and the ablated material was removed by an exhaust.

3 Results and Discussion

3.1 Screen printed Cr-Ni electrode

Figure 3 shows SEM images of a Cr-Ni electrode for alkaline fuel cells screen printed onto carbon substrate. The Cr-Ni particle size is estimated to be in the range of 10 -50 µm as observed from Fig. 3 left with magnification 50 µm and 10 µm on the right side. The particles are interconnected and well attached to the porous carbon paper substrate. Furthermore, the texture of the coating exhibits pores which are necessary for proper operation of the fuel cell. This type of electrode constitution was used for performing ultrafast laser ablation experiments.

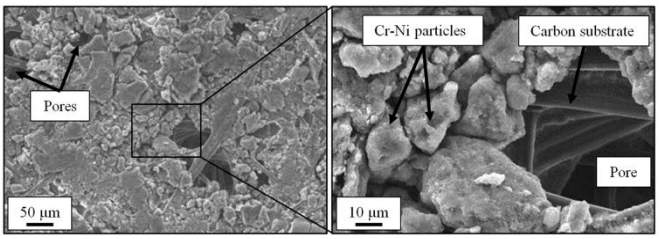

Fig. 3: Top-view SEM images of a Cr-Ni electrode surface.

3.2 Laser structured Cr-Ni electrode for alkaline fuel cells

3D microstructures were formed in Cr-Ni electrodes by applying an fs-laser ablation process. A schematic of a similar laser scanning strategy is described elsewhere [21]. The pitch in between to laser scans was maintained at 100 µm for both 3D micro-grids (Fig. 4) and 3D micro-channels (Fig. 5).

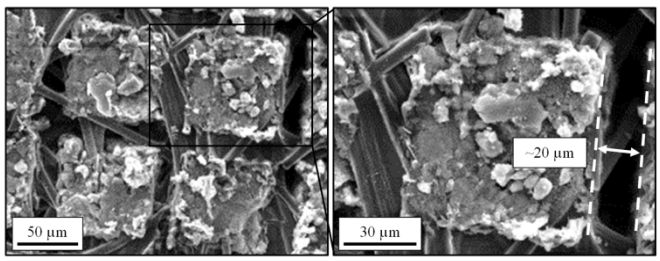

Fig. 4: Top-view SEM image of laser generated micro-grids in Cr-Ni electrode.

Micro-grid structures could be formed with a distance of about 20 µm in between two 3D features (Fig. 4). The Cr-Ni electrode could be completely removed from the laser beam interaction zone and no impact to or damage of the carbon substrate could be detected (Fig. 4 and 5).

Besides natural pores resulting from the screen printing process, a laser-induced artificial porosity could be achieved by removal of the electrode material down to the carbon substrate for both 3D micro-grids (Fig. 4) and 3D micro-channel features (Fig. 5). In general, the Cr-Ni electrode material and the carbon substrate are in contact with liquid electrolyte, e.g. KOH (pH = 14) during fuel cell operation and therefore, complete electrode wetting is aspired. Sufficient electrode wetting is known to be essential and has already been influenced for porous composite electrode materials for lithium-ion batteries whereby improved electrolyte wetting could be achieved for both 3D micro-grids [21,22] and 3D micro-channel structures [23,24]. Furthermore, similar distances of 15 - 22 µm in between two micro-features could be achieved for Cr-Ni electrodes for alkaline fuel cells as well as for composite electrodes for lithium-ion batteries by applying fs-laser ablation processes [21].

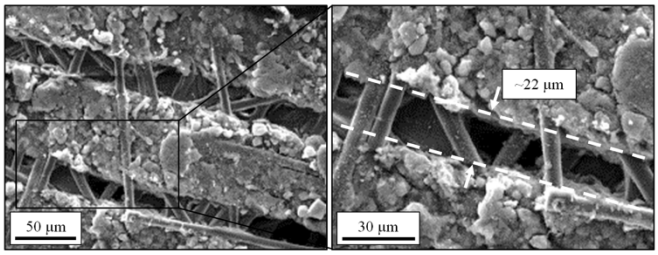

Fig. 5: Top-view SEM images of laser-generated micro-channels in Cr-Ni electrode.

In general the aim is to increase the exchange current density of electrode materials for fuel cells. Therefore, an enhanced reaction surface A is required. With a distance of about $g = 20$ µm in between two laser-generated 3D grid structures and a height of a single microstructure of about $h = 25$ µm, the increased reaction surface A for 3D micro-grids could be estimated by the following equation:

$$A = [(a/n - g)^2 + 4 \cdot (a/n - g) \cdot h)] \cdot n^2, \qquad (1)$$

whereby $a = 5$ cm describes the edge length of the electrode footprint and n an integral factor. Within this work, the skin surface of laser-generated 3D micro-grids (Fig. 4) could be increase by ~ 30 % compared to an unstructured electrode.

4 Conclusion

Cr-Ni electrode material for application in alkaline fuel cells was prepared and screen printing onto carbon paper substrate.. The coated electrode was pressed in order to improve the contact of the electrode to the substrate and to unitize the film thickness. Within a first approach, 3D micro-features such as grid and channel structures could be formed into the electrode by applying an ultrafast laser structuring processes. The distance in between two microstructures was determined to 20 - 22 µm. Laser structuring of Cr-Ni electrodes resulted in artificial porosity and an enhanced skin surface of 3D grids of up to 30 %. Further investigations will focus on measurement of exchange current density as well as the influence of the microstructure on the power density completed with the verification of the theoretical analyzes.

Therefore, different geometries for 3D structures and a resulting variation in active skin surfaces will be tested by adjusting the aspect ratio of 3D features with respect to electrode film thickness and laser processing parameters. The investigation of the correlation of these parameters will allow the design of optimized 3D features in electrode materials with improved exchange current density.

ACKNOWLEDGEMENT

This work was supported by the Berthold Leibinger Stiftung as a carrier of the Fritz-Hüttinger scholarship. Finally, the support for laser processing by the Karlsruhe Nano Micro Facility (KNMF, http:// www.knmf.kit.edu) a Helmholtz research infrastructure at the Karlsruhe Institute of Technology is gratefully acknowledged.

REFERENCES

1. C. Bretthauer, C. Müller, H. Reinecke., "A precious-metal free micro fuell cell accumulator," Journal of Power Sources 196 , pp. 4729–4734, 2011.
2. G. McLean., "An assessment of alkaline fuel cell technology," International Journal of Hydrogen Energy 27, pp. 507–526. 2002.
3. S. Trasatti., "Electrocatalysis understsnding the success of DSA," Electrochimica Acta 45, pp. 2377–2385. 2000
4. A.J. Bard, R. Parsons, J. Jordan., "Standard potentials in aqueous solution, 1st ed. Monographs in electroanalytical chemistry and electrochemistry," M. Dekker, New York, 1985.
5. P. Anderson., "Localized Magnetic States in Metals," Phys. Rev. 124, pp. 41–53, 1961.
6. E. Santos, W. Schmickler., "Electrocatalysis of Hydrogen Oxidation-Theoretical Foundations," Angew. Chem. Int. Ed. 46, pp. 8262–8265, 2007.
7. A. Prieto, J. Hernandez, E. Herrero, J.M. Feliu., Journal of Solid State Electrochemistry 7, pp. 599–606, 2003
8. Xianfeng Dai1, Jinli Qiao1,*, Xuejun Zhou1, Jingjing Shi1, Pan Xu1, Lei Zhang2, Jiujiun Zhang2, "Effects of Heat-Treatment and Pyridine Addition on the Catalytic Activity of Carbon-Supported Cobalt-Phthalocyanine for Oxygen Reduction," International Journal of Electrochemical Science , 2013.
9. R.D.L. Smith, M.S. Prevot, R.D. Fagan, Z. Zhang, P.A. Sedach, M.K.J. Siu, S. Trudel, C.P. Berlinguette., "Photochemical Route for Accessing Amorphous Metal Oxide Materials for Water Oxidation Catalysis," Science 340, pp. 60–63, 2013.
10. H.A. Gasteiger, S.S. Kocha, B. Sompalli, F.T. Wagner., "Activity benchmarks and requirements for Pt, Pt-alloy, and non-Pt oxygen reduction catalysts for PEMFCs," Applied Catalysis B: Environmental 56, pp. 9–35, 2005.
11. Y. Gorlin, T.F. Jaramillo., "Investigation of Surface Oxidation Processes on Manganese Oxide Electrocatalysts Using Electrochemical Methods and Ex Situ X-Ray Photoelectron Spectroscopy," Journal of the Electrochemical Society 159, pp. H782–H786, 2012.
12. Y. Gorlin, T.F. Jaramillo., "A Bifunctional Nonprecious Metal Catalyst for Oxygen Reduction and Water Oxidation," J. Am. Chem. Soc. 132, pp. 13612–13614, 2010.
13. M. Chigane, M. Ishikawa., "Manganese Oxide ThinFilm Preparation by Potentiostatic Electrolyses and Electrochromism," J. Electrochem. Soc. 147, pp. 2246, 2000.
14. M. Chigane, M. Ishikawa, M. Izaki., "Preparation of manganese Oxide Thin Films by Electrolysis/Chemical Deposition and Electrochromism," J. Electrochem. Soc. 148, pp. D96, 2001.
15. B. de Mishima, T. Ohtsuka, N. Sato., "In-situ raman spectroscopy of manganese dioxide during the discharge process," Journal of Electroanalytical Chemistry and Interfacial Electrochemistry 243, pp. 219–223, 1988.
16. B. de Mishima, T. Ohtsuka, H. Konno, N. Sato., "XPS study of the MnO2 electrode in borate solution during the discharge process," Electrochimica Acta 36, pp. 1485–1489, 1991.
17. M. Zaw., "Speciation if iron and manganese in dam water particles using electron spectroscopy for chemical analysis (ESCA)," Talanta 42, pp. 27–40, 1995.
18. R.A. Marcus., "On the Theory of Oxidation-Reduction reactions Involving Electron Transfer," J. Chem. Phys. 24, pp. 966, 1956.
19. N.S. Hush., "Adiabatic Rate Processes at Electrodes," J. Chem. Phys. 28, pp. 962, 1958.
20. S. Lu, J. Pan, A. Huang, L. Zhuang, J. Lu, Proceedings of the National Academy of Sciences 105 (2008) 20611–20614., P., "Localized Magnetic States in Metals," Phys. Rev., vol. 124, no. 1, pp. 41–53, 1961.
21. J. Pröll, H. Kim, A. Piqué, H.J. Seifert, W. Pfleging., "Laser-printing and femtosecond-laser structuring of $LiMn_2O_4$ composite cathodes for Li-ion microbatteries," J. Power Sources 255, pp. 116-124, 2014.
22. J. Pröll, H. Kim, M. Mangang, H.J. Seifert, A. Piqué, W. Pfleging., "Fs-laser microstructuring of laser-printed $LiMn_2O_4$ electrodes for manufacturing of 3D microbatteries," Proc. of SPIE Vol. 8968, pp. 896805-1-896805-6, 2014, doi: 10.1117/12.2039902, ISBN: 978-0-8194-9881-6.
23. W. Pfleging, J. Pröll., "A new approach for rapid electrolyte wetting in tape cast electrodes for lithium-ion batteries," J. Mater. Chem. A 2, pp. 14918-14926, 2014.
24. W. Pfleging, R. Kohler, J. Pröll., "Laser generated microstructures in tape cast electrodes for rapid electrolyte

wetting – new technical approach for cost efficient battery manufacturing (2014 Green Photonics Best Paper Award), " Proc. of SPIE Vol. 8968, pp. 89680B-1-89680B-8, 2014, doi: 10.1117/12.2039635, ISBN: 978-0-8194-9881-6.